# State-Space Model Representation to Characterize an Energy Harvesting Circuit

Regis Rousseau, Guillaume Villemaud, Florin Hutu

# State-Space Model Representation to Characterize an Energy Harvesting Circuit

*Regis Rousseau, Guillaume Villemaud, and Florin Hutu*

*Abstract* – This paper presents a method to model an energy harvesting circuit and a propagation channel as parts of a wireless power transfer (WPT) system. Previously, an original solution was proposed by the authors to maximize the collected DC power level, implying to model the different parts of the system by using state space representation and using convex optimization algorithms to calculate multi carrier signal weights. Firstly, a state-space model of the radio channel is obtained by the use of multivariable output-error state space (MOESP) algorithm. Then, by the vector fitting method a state-space representation is obtained in order to model the linear part of the energy harvesting circuit. At last, by the polynomial-nonlinear state-space (PNLSS) method, the non-linear part of the rectifier is also modeled.

## 1. Introduction

For several years now, research has been undertaken to maximize the DC harvested power obtained by an energy harvesting circuit. The use of multi-tone signals has shown their impact in terms of increasing performance. This article presents the scientific advances in this field and the challenges for tomorrow [1]. In the case of power transfer, [2] has shown that the use of power-optimized waveform (POW) considerably impacts the efficiency of the rectifier. With an optimal range of the sub-carrier spacing, the voltage ripple and the total number of sub-carriers, a relationship has been established in order to maximize the efficiency of a single-shunt rectifier. POW is a solution to increase the peak-to-average power ratio (PAPR) of the transmitted source signal and thus to deliver more power to the load. Since peaks of high power drive the rectifier with a much higher efficiency than the average low level input, they contribute more to the output DC voltage. But some trade-off appear like the frequency spacing between sub-carriers and their number with regard to the bandwidth of matching network.

However, this concerns only the rectifier's physical characteristics. Nowadays, the trend is to take also into account the transmission channel's characteristics. The radio-frequency source (multi-sine), the channel and the rectifier are considered as a global WPT system. The authors in [3] described the influence of a realistic channel on the WPT system's overall efficiency. The presented measurements show that the power conversion efficiency (PCE) is always better in the case of a single-path channel. On the other hand, having a precise knowledge of the channel, as for instance the coherence bandwidth, will be crucial in the choice of the number of tones and the frequency bandwidth of the transmitted RF signal.

Waveform tailoring algorithms according to the characteristics of the propagation channel have thus been developed [4] and experimentally verified [5]. In these study cases, the rectifier only consists of a model based on I-V characteristic law of a Schottky diode [6]. Other works concern rectifier model extraction based on curve fitting [7]. The DC output power as a function of RF input level is measured and this characteristic is approximated from simulation data using a data-fitting tool. Several nonlinear curve-fitting models are currently used like second-order polynomial model, sigmoid model, and rational function model. In these solutions, the rectifier is considered ideal and depends only on the model of Schockley's law or is modeled by a neighboring polynomial. Those adaptive and optimized waveforms use non-convex optimization problems, therefore the implementation is complex.

In this paper, we describe a possible way of closed loop modeling of a WPT system by using linear and nonlinear state-space models. In a second time, the use of convex optimization algorithms will be employed in order to maximize the DC power harvested in a WPT scenario. Three main aspects of a WPT system are taken into account: the RF multi-sine source, the propagation channel and the rectifier in its entirety. Each of its elements finds its representation in a state-space model and the algorithm optimization will become a convex optimization resolution. This work describes different algorithms to represent by state-space model a global system of WPT. The first part shows the global system and the goal of this approach, the second part shows the state-space model of a frequency-selective channel knowing the channel state information, and the last part describes the state-space model of linear and nonlinear part of the rectifier.

## 2. Global System Model

The initial scenario foresees a wireless power supply from a source to a connected object equipped with a rectenna which will ensure the charging of an external storage element (battery or super-capacitor). This study

case rather provides a scenario of an indoor condition with non-line-of-sight (NLOS) or line-of-sight (LOS) environments and with short distances (few meters). As detailed in [11], the global system is seen as a closed-loop WPT system and is put in the form presented in Figure 1. The channel is considered to be linear and the rectifier, by the presence of the rectifying diode, is considered to be nonlinear, so their models do not use the same shaping algorithm and are thus treated distinctly.

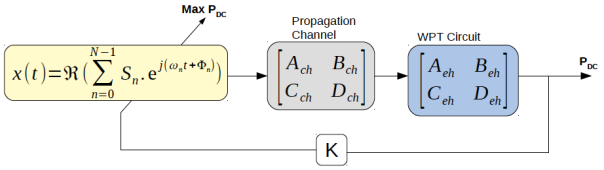


Figure 1: A WPT system seen as a closed loop. Propagation channel and rectifying circuit are modeled by their respective state-space models.

Before generating the adaptive waveform, the RF source generates a reference orthogonal frequency-division multiplexing (OFDM) signal in order to know the channel estimation in amplitude and phase. Knowing beforehand the electrical characteristics of the rectifier and put them in a form of state-space model, an algorithm computes the channel state information on state-space model. A closed-loop is created and an optimized waveform can be generated.

## 3. Frequency-Selective Channel Model

First of all, a static wireless multi-path channel between the source and the rectifier is simulated. As mentioned in [3], the source node transmits multi-sine signals to the receiver via a multi-path channel with gain $\beta_k$ and delay $\tau_k$ for the $k_{th}$ path. Starting from this, we assume that the transmitter, receiver and the channel environment are stationary during the observation time. The considered frequency-selective channel corresponds to NLOS channel power delay profile scenario with a root mean square (RMS) delay spread of 100 ns, a coherence bandwidth of 5 MHz and terminal speed of 3 m/s (equivalent to a channel model B for HYPERLAN/2 [8]).

The channel estimator process uses block-pilot based technique. Leveraging channel estimation for OFDM, we can therefore collect the channel state information (CSI) on each frequency. The pilot-based technique uses a reference pilot signal that the transmitter and the receive both know. The channel status information can be calculated from comparison between received signal and known reference signal at the receiver. Pilot symbols are allocated one frequency out of 2. Also, we use a least-square (LS) method to calculate the CSI because of its low complexity. Our channel estimation system operates at 2.45 GHz center frequency with a 20MHz bandwidth and 256 subcarriers, corresponding to a subcarrier spacing of 78.125 kHz. However, the upper and lower 5MHz bands are used as guard bands, and the region that is actually used to estimate the channel is the middle one of 10 MHz.

From the simulated input/output of the channel, the state-space model is computed by a system identification based on Multivariable Output-Error State sPace (MOESP). MOESP is a deterministic method to identify linear time invariant systems. The MOESP method developed cited in [9] is based on the LQ decomposition of Hankel matrix formed from input/output data, where L is lower triangular matrix and Q is orthogonal one. A Singular Value Decomposition (SVD) can be performed on a block from the L matrix to obtain the system order and the extended observability matrix. From this matrix, it is possible to estimate the matrices C and A of state-space model. The final step is to solve overdetermined linear equations using the least-square method to calculate matrices B and D. Figure 2 shows the comparison of the magnitude of the frequency response of the wireless channel from CSI and the magnitude of the frequency response from space-state model. The RMS frequency response error of the MOESP model on the estimation data is 0.5908.

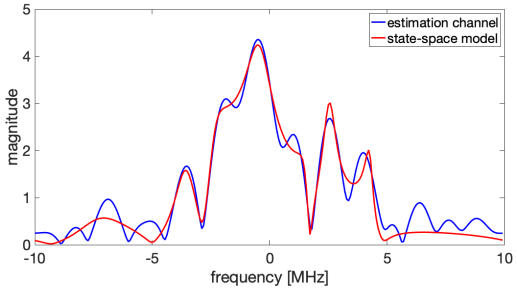


Figure 2: Magnitude of the frequency response from impulse response of the estimated channel (blue) and from the MOESP method with order 10 (red). The bandwidth of the channel is 20MHz with 10MHz guard band.

## 4. Rectifier Model

Since the forecast scenario concerns very low received powers (approx. -40 dBm), a rectifier with a single diode was retained. The single shunt diode rectifier circuit is designed by using a Skyworks SMS7630 Schottky diode. The rectifier input is matched to 50Ω by two L-matching networks (6-order LC bandpass filter). It guarantees an input reflection coefficient between -20dB and -33dB for an input signal of 2.45GHz having a 60MHz

Table 1: Voltage and efficiency results

| *Pin* [dBm] | *DC Voltage* [mV] | *Efficiency* [%] |
|---|---|---|
| -40 | 0.002 | 1.6 |
| -30 | 0.089 | 10 |
| -20 | 3.613 | 36 |
| -10 | 63.195 | 56 |

bandwidth and a -20dBm input power level (all values were optimized and normalized in previous studies). The load resistance is optimized with the same optimization criteria concerning the input reflection coefficient and its value is 3953Ω. Table 1 gives some reference performance values of this proposed rectifier for a continuous wave (1-tone). The maximum efficiency is obtains for an input power level of -9.5 dBm, its value is 52.5 % for a DC output voltage of 58.91 mV.

These results are in good agreement with the literature. In [10], an experimental rectifier is presented with a similar rectifier topology. The measured peak efficiencies are respectively 4.3%, 24.3%, 48.5% with an input power level of -30, -20, -10 dBm at the frequency of 2.472 GHz. Therefore our goal is also to maximize DC output voltage for input power below -30dBm by knowing the distortion of the channel.

### 4.1. Impedance Matching Network Model

In [11], the authors shows that by using the vector fitting method, a linear time-invariant system can be computed in a form of state-space model. A description for the S-parameter based-model is given in [12]. We employed this method to approximate the linear impedance matching network (IMN) seen like a quadripole by a rational function. S-parameters of IMN (6-order LC bandpass filter) can then be modeled as a sum of the residues, $r_k$, over first-order poles, $p_n$: $H(s) = \sum_{k=1}^{N} \frac{r_k}{s-p_k} + d = C(s.\mathbb{I} - A)^{-1}B + D$ where N denotes the VF order and s = j$\omega$. Considering a 2-port (n = 2) system and VF of order N = 5, the total number of state variables m will be m = n.N = 10. Thus, the corresponding state-space model will have the following properties: A is an 10x10 diagonal matrix containing the N poles $p_k$ repeated 2 times, B is an 10x2 matrix and contains only ones or zeros, C is composed of the $r_k$ residues and is an 2x10 matrix, and D is a 2x2 matrix and is composed of real constants. Figure 3 shows the input reflection coefficient as function of frequency, from 2.4 GHz to 2.5 GHz for N = 5 and an input power of -20dBm. As can be seen, the model for an order of 5 gives a similar response than the original model.

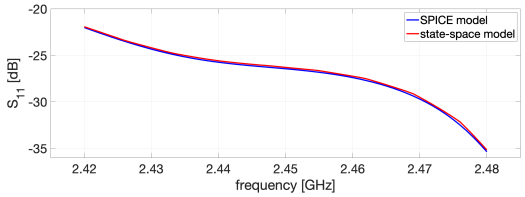


Figure 3: In blue, the reflection coefficient (in dB) of the original rectifier. In red, the reflection coefficient from VF method, order 5.

### 4.2. DC Behavior Diode Model

As previously stated, the Schottky diode SMS7630-001LF is selected for the rectifier due to its small series resistance (20Ω) and its small junction potential (0.34 V). The first step is to model its DC characteristic under reverse-bias and forward-bias. The objective of this step is to model the nonlinear junction resistance as a polynomial equation. The characteristic was obtained using its electric circuit in the range of -300 mV to +300 mV. Then, the DC behaviour was represented by a symbolically defined device (SDD) element which takes the form of a polynomial equation $I_d = f(V_d)$ of order 9, where Id denotes the current through the diode and $V_d$ denotes the voltage across the diode. Figure 4 shows comparison of spice model simulated and polynomial fitting of the I-V characteristic. The correlation is intended to be very good for low voltage values, but beyond 50 mV, an error will appear to be significant as it increases. However, the target values being low, this model can be used since the objective is to recover low power level at the input of the rectifier.

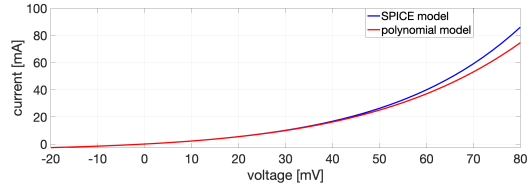


Figure 4: In blue, the original I-V characteristic. In red, the I-V characteristic from polynomial fitting, order 9.

### 4.3. RF Behavior Diode Model

To model the RF behaviour of the diode from -300 mV to +300 mV, the nonlinear junction capacitance was also represented by an SDD element. This capacitance value is driven by the voltage Vd across it, based on $C_j = 0.14 \cdot 10^{-12} \cdot e^{(Vd)}$. The same method has been applied to put this equation in the form of a polynomial of order 7. The SDD models a nonlinear voltage-controlled capaci-

tor, whose the current can be written $Id = Cj(Vd).\frac{dVd}{dt}$. The time derivative is implemented in the SDD by specifying weighting function number 1. Figure 5 shows the comparison between the simulated electrical circuit and the simulated polynomial fitting model. This curve shows that the modeling of the nonlinear capacitance of the diode by this exponential function perfectly meets this need for a modeling in polynomial form. The curve resulting from the polynomial model is coincided with the original spice model over the entire frequency range.

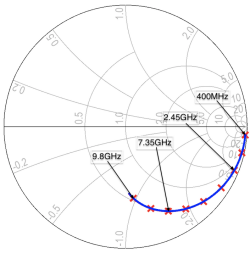


Figure 5: $S_{11}$ parameter for a frequency range from 400MHz to 9.8GHz. In blue, the original $S_{11}$ parameter. In red, the obtained polynomial fitting.

### 4.4. Polynomial Nonlinear State-Space Model

From now on the rectifier can be entirely modeled by functional blocks given as state-space models. Their state-space model result from the VF methods for the linear parts (impedance matching network and input/output SOT-23 parasitic parts), the non-linear components being replaced by SDD elements. Figure 6 shows comparison of the rectifier's DC collected voltage as a function of the RF input power between the original rectifier and the fully modeled rectifier. The model is faithful to the original for powers below -20 dBm. Then, while the voltage from the original increases, saturation seems to appear concerning the rectifier from the models. Nevertheless, our target is there low received power, so this model is perfectly appropriate for operation below -20dBm.

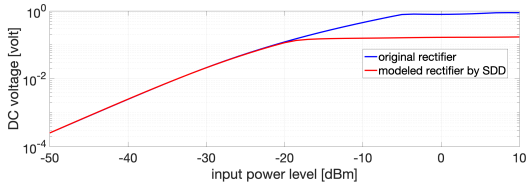


Figure 6: In blue, the original rectifier. In red, the modeled rectifier.

The last step in order to completely model this rectifier with state-space model is to replace these SDD elements with their own nonlinear state-space representation. This representation is carried out by the use of an original method presented [13] and Matlab functions in [14]. The state and output equation of the model are given by:

$$\begin{cases} \dot{x} = A \cdot x + B \cdot u + E \cdot f(x(t), u(t)) \\ y = C \cdot x + D \cdot u + F \cdot g(x(t), u(t)) \end{cases} \quad (1)$$

where $\dot{x}$ is the time derivative operator of the state variable, $u$ is the input vector of length $N$, $y$ is the corresponding output vector of length $P$. The state vector has the length $N$.

The matrix $A$ is the $N \times N$ state matrix, $B$ is the $N \times M$ input matrix, $C$ is the $P \times N$ output matrix, and $D$ is the $P \times N$ feedback matrix. The $f(x(t), u(t))$ and $g(x(t), u(t))$ functions are multivariate and monomial, the matrices $E$ and $F$ contain the corresponding coefficients. The model is established in 3 steps: an estimation of the best linear approximation (BLA), an estimation of a subspace model, and an optimization of the model parameters.

Figure 7 shows the output resulting by a DC voltage input from PNLSS model and the Spice model. The RMS output error of the best PNLSS model on the estimation data is $2.10^{-5}$. However, this error is minimal for weak inputs and tends to increase for larger values. Future work will therefore be granted in order to improve the precision.

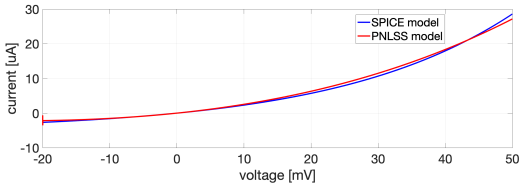


Figure 7: In blue, the original I-V characteristic. In red, the I-V characteristic from PNLSS model, order 2.

## 5. Conclusion

This paper proposes strategies in order to extract state-space representations of the different building blocks of a wireless power transfer system. More in details, the proposed strategy includes one algorithm to compute a CSI impulse response to a state-space model and two distinct algorithms to compute the linear and the nonlinear part of the rectifier. Future work will focus on putting the state-space model representations in the form of a closed-loop and proposing an optimization algorithm for the adaptive input waveform. Moreover, a work will be carried out in order to reduce the order of the rectifier's model.

## 6. References


1. COST Action IC1301 Team, "Europe and the Future WPT", *IEEE Microwave Magazine*, **18**, 4, June 2017, pp. 56-87.
2. C. R. Valenta and G. D. Durgin, “Harvesting Wireless Power,” *IEEE Microwave Magazine*, **15**, 4, June 2014, pp. 108-120.
3. N. Pan, M. Rajabi, D. Schreurs and S. Pollin, “Multi-sine Wireless Power Transfer with a Realistic Channel and Rectifier Model,” *IEEE Wireless Power Transfer Conference*, June 2017.
4. B. Clerckx and E. Bayguzina, “Waveform Design for Wireless Power Transfer,” *IEEE Transaction on Signal Processing*, **64**, 23, March 2016, pp. 6313 - 6328.
5. J.Kim, B. Clerckx and P D. Mitcheson, “Prototyping and Experimentation of a Closed-Loop Wireless Power Transmission with Channel Acquisition and Waveform Optimization,” *IEEE Wireless Power Transfer Conference*, May 2017.
6. B. Clerckx, R. Zhang, R. Schober and D. Wing Kwan Ng, "Fundamentals of Wireless Information and Power Transfer: From RF Energy Harvester Models to Signal and System Designs," *IEEE Journal on Selected Areas in Communications*, **37**, 1, January 2019.
7. B. A Mouris, H. Ghauch, R. Thobaben and B. L. G. Jonsson, "Multi-tone Signal Optimization for Wireless Power Transfer in the Presence of Wireless Communication Links," *IEEE Transactions on Wireless Communications*, **19**, 5, May 2020, pp. 3575 - 3590.
8. J. Medbo and P. Schramm, "Channel Models for HIPERLAN/2 in Different Indoor Scenarios", *ETSI EP BRAN*, March 1998.
9. J. N. Juang and M. Q. Phan, "Identification and Control of Mechanical Systems," *Cambridge University Press*, 2001.
10. Yong Huangl, Naoki Shinoharal and Hiroshi Toromura, ”A Wideband Rectenna for 2.4 GHz-band RF Energy Harvesting”, *IEEE Wireless Power Transfer Conference*, June 2016.
11. R. Rousseau, F. Hutu and G. Villemaud,"On the Use of Vector Fitting and State-Space Modeling to Maximize the DC Power Collected by a Wireless Power Transfer System," *2nd URSI Atlantic Radio Science Conference*, May 2018.
12. B. Gustavsen and A. Semlyen, "Rational approximation of frequency domain responses by vector fitting," *IEEE Transaction Power Delivery*, **14**, 3, July 1999, pp. 1052-1061.
13. J. Paduart, L. Lauwers, J. Swevers, K. Smolders, J. Schoukens, and R. Pintelon, “Identification of Nonlinear Systems using Polynomial Nonlinear State Space models,” *Automatica*, **46**, 4, April 2010, pp. 647-656.
14. K. Tiels,"A Polynomial Nonlinear State-Space Toolbox for Matlab", *21th IMEKO TC4 International Symposium on Understanding the World through Electrical and Electronic Measurement*, September 2016.



Regis Rousseau is with INSA Lyon, CITI laboratory-INRIA, 6 avenue des arts, F-69621 Villeurbanne, France; e-mail: regis.rousseau@insa-lyon.fr.

Guillaume Villemaud is with INSA Lyon, CITI laboratory-INRIA, 6 avenue des arts, F-69621 Villeurbanne, France; e-mail: guillaume.villemaud@insa-lyon.fr.

Florin Hutu is with INSA Lyon, CITI laboratory-INRIA, 6 avenue des arts, F-69621 Villeurbanne, France; e-mail: florindoru.hutu@insa-lyon.fr.